Temporary Anion States and Dissociative Electron Attachment in Diphenyl Disulfide

Alberto Modelli*,† and Derek Jones‡

Dipartimento di Chimica "G. Ciamician", Università di Bologna, via Selmi 2, 40126 Bologna, Italy, Centro Interdipartimentale di Ricerca in Scienze Ambientali (CIRSA), Università di Bologna, via S. Alberto 163, 48100 Ravenna, Italy, and ISOF, Istituto per la Sintesi Organica e la Fotoreattività, C.N.R., via Gobetti 101, 40129, Bologna, Italy

Received: May 10, 2006; In Final Form: June 16, 2006

The temporary anion states of gas-phase diphenyl disulfide are characterized by means of electron transmission (ET) and dissociative electron attachment (DEA) spectroscopies. The measured energies of vertical electron attachment are compared to the virtual orbital energies of the neutral state molecule supplied by MP2 and B3LYP calculations with the 6-31G* basis set. The calculated energies, scaled with empirical equations, reproduce satisfactorily the attachment energies measured in the ET spectrum. The first anion state of diphenyl disulfide is stable, thus escaping detection in ETS. The vertical and adiabatic electron affinities, evaluated with B3LYP/6-31+G* calculations as the energy difference between the neutral and anion states, are predicted to be 0.37 and 1.38 eV, respectively. The anion current displayed in the DEA spectrum has a sharp and intense peak at zero energy, essentially due to the $C_6H_5S^-$ negative fragment. In agreement, according to the calculations, the localization properties of the first anion state are strongly S−S antibonding, and the energetic requirement for its dissociation along the S−S bond is fulfilled even at zero energy.

Introduction

Because of its electronic properties, sulfur plays a major role in a variety of metabolic processes and, more in general, in the chemistry of life. In particular, S−S bridges between cysteines are present in the amino acid backbone of proteins. Disulfide bonds are involved in conformational stability and biological activity of proteins and in protein folding. The formation of disulfide bonds is catalyzed by protein disulfide isomerases, which also display chaperone activities.[1] The recently discovered Hsp33 protein, which functions as a highly efficient molecular chaperone, protects bacterial cells against oxidative stress, and its activation process is accompanied by the formation of intramolecular disulfide bonds.[2] Reduction of disulfide bonds is involved in many biochemical mechanisms. Molecular dynamics techniques have indicated that the native conformation of lysozyme evolves toward unfolded conformations upon reduction of disulfide bonds.[3] Light generates reducing equivalents that are used for the activity of chloroplast enzymes by reduction of regulatory disulfides via the ferredoxin:thioredoxin reductase system.[4] Cellular redox status, which regulates fundamental cellular functions, is maintained by intracellular molecules, such as the small thermostable protein thioredoxin, through a redox-active disulfide/dithiol couple.[5,6] Protein disulfur radical anions may decay following different paths through competing intra- and intermolecular routes, including bond cleavage, disproportionation, protein−protein cross linking, and electron transfer.[7] Mass spectrometry studies have shown that capture of low-energy (<0.2 eV) electrons by multiply protonated proteins is followed by dissociation of S−S bonds holding two peptide chains together.[8]

The study of the electron-acceptor properties of disulfides in the gas phase and characterization of their lowest-lying anion states may serve as a model for the understanding of the reductive process in larger biological systems.

Such studies are also important for a greater understanding of the processes occurring when thiols and disulfides are used for tethering organic molecules containing conjugated π systems to surfaces without too much perturbation of those π systems. For example, both benzenethiol and diphenyl disulfide have been used to bond benzene systems to silicon[9] as part of recent intense research activity aimed at the production of hybrid silicon−organic molecule nanoelectronics devices.[10]

Electron transmission spectroscopy (ETS)[11] is one of the most suitable means for detecting the formation of gas-phase temporary anion states. Because electron attachment is rapid with respect to nuclear motion, anions are formed with the equilibrium geometry of the neutral molecule. The impact energies at which electron attachment occurs are properly denoted as vertical attachment energies (VAEs) and are the negative of the vertical electron affinities. Both the physical process and the corresponding structures observed in the electron−molecule scattering cross-section are referred to as resonances.

Additional information can be supplied by dissociative electron attachment spectroscopy (DEAS),[12] which measures the yield of negative fragments, as a function of the impact electron energy. When suitable energetic conditions occur, the decay of unstable molecular anions formed by resonance can follow a dissociative channel, which generates negative fragments and neutral radicals, in kinetic competition with simple re-emission of the extra electron:

$$e^-_{(E)} + AX \rightarrow AX^-{}^* \rightarrow A + X^-$$

The lifetime of the negative fragments produced is usually sufficiently long to allow their detection by means of a mass filter. Measurements of the negative ion abundance as a function

* Corresponding author. Telephone: +39 051 2099522. Fax: +39 051 2099456. E-mail: alberto.modelli@unibo.it.
† Università di Bologna.
‡ ISOF.

10.1021/jp0628683 CCC: $33.50
Published on Web 08/09/2006

of the incident electron energy thus give insight into the nature and efficiency of the dissociative channels of resonance processes.

The ET spectrum of dimethyl disulfide displays the first resonance at 1.04 eV, associated with vertical electron attachment to the lowest unoccupied molecular orbital (LUMO) with mainly σ^* (S−S) character.[13] The DEA spectra show that this resonance generates negative fragments due essentially to dissociation of the S−S bond, the abundance of fragments due to dissociation of S−C bonds being 3 orders of magnitude smaller.[13] More recently, a Rydberg electron-transfer and negative ion photoelectron spectroscopy study[14] indicated that the geometrically relaxed ground anion state of the saturated disulfides RS−SR (R = methyl, ethyl, propyl) is slightly stable (0.1 eV); that is, the adiabatic electron affinity (AEA) is slightly positive.

In diphenyl disulfide, mixing of the empty σ^*_{S-S} MO with the benzene π^* MOs is expected to stabilize the lowest-lying anion state with respect to that of the saturated disulfides, thus simulating more closely the electron-acceptor properties of the S−S bond in the positively charged proteins. However, it is not a priori obvious whether the ground anion state possesses mainly σ^*_{S-S} or ring π^* character.

In the present multidisciplinary approach, diphenyl disulfide is analyzed by means of ET and DEA spectroscopies and theoretical calculations to characterize the energetics of electron attachment and obtain insight into the dissociative decay channels of the observed temporary anion states. B3LYP and MP2 calculations are employed to describe the nature of the singly occupied MO (SOMO) of the ground anion state, the localization properties of the extra electron playing an important role in determining the position of bond cleavage in the process of anion dissociation.

Experimental Section

Our electron transmission apparatus is in the format devised by Sanche and Schulz[11] and has been previously described.[15] To enhance the visibility of the sharp resonance structures, the impact energy of the electron beam is modulated with a small ac voltage, and the derivative of the electron current transmitted through the gas sample is measured directly by a synchronous lock-in amplifier. Each resonance is characterized by a minimum and a maximum in the derivative signal. The energy of the midpoint between these features is assigned to the vertical attachment energy (VAE). The present spectrum has been obtained by using the apparatus in the "high-rejection" mode[16] and is, therefore, related to the nearly total scattering cross-section. The electron beam resolution was about 50 meV (fwhm). The energy scale was calibrated with reference to the $(1s^12s^2)^2S$ anion state of He. The estimated accuracy is ±0.05 or ±0.1 eV, depending on the number of decimal digits reported.

The collision chamber of the ETS apparatus has been modified[17] to allow for ion extraction at 90° with respect to the electron beam direction. Ions are then accelerated and focused toward the entrance of a quadrupole mass filter. Alternatively, the total anion current can be collected and measured with a picoammeter at the walls of the collision chamber (about 0.8 cm from the electron beam). Measurements of the total anion current were obtained with an electron beam current about twice as large as that used for the ET experiment. The energy spread of the electron beam increased to about 120 meV, as evaluated from the width of the SF_6^- signal at zero energy used for calibration of the energy scales.

Calculations were performed with the Gaussian 98 set of programs.[18] The first VAE was calculated as the difference of the total energy of the neutral and the lowest anion state, both in the optimized geometry of the neutral state, using the B3LYP hybrid functional[19] with the standard 6-31G* and 6-31+G* basis sets. The adiabatic electron affinity (AEA) was obtained as the energy difference between the neutral and the lowest anion state, each in its optimized geometry. Evaluation of the virtual orbital energies (VOEs) of the neutral molecule was performed at the second-order many-body perturbation theory (MP2) and B3LYP levels with the 6-31G* basis set.

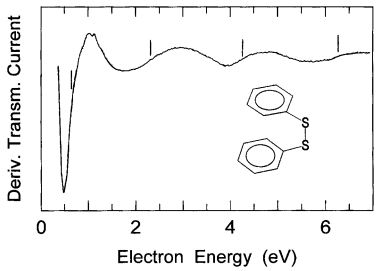

Figure 1. Derivative of transmitted current, as a function of the incident electron energy, in diphenyl disulfide.

Results and Discussion

Electron Transmission Spectrum and Calculated VAEs. The ET spectrum of diphenyl disulfide in the 0−7 eV energy range is reported in Figure 1. Resonances are displayed at 0.63, 2.3, 4.28, and 6.2 eV. The VAEs measured in the ET spectra of the reference molecules benzene[15] (1.12 eV, π^* e_{2u}; 4.82 eV, π^* b_{2g}) and dimethyl disulfide[13] (1.04 eV, σ^*_{S-S}; 2.72 eV, σ^*_{S-C}) indicate that in diphenyl disulfide electron capture into the six empty ring π^* MOs and three lowest-lying σ^* MOs is expected to occur at energies lower than 6 eV. Thus, a first qualitative analysis suggests that the signal centered at 4.28 eV should arise from the unresolved contributions of both the two highest-lying benzene π^* MOs, electron attachment to the two σ^*_{S-C} MOs is likely accounted for by the broad signal at 2.3 eV, and the signal at 0.63 eV should be associated with two or three (close in energy) π^* MOs (deriving from the benzene e_{2u} LUMO). Finally, the ground anion state (stabilized by σ^*_{S-S}/π^* mixing) could possibly lie very close to zero energy (where it would be hidden by the intense electron beam signal) or be stable (thus not accessible in ETS). The feature centered at 6.2 eV is thus likely due to a core-excited resonance, that is, a two-particle process where electron capture is accompanied by simultaneous excitation of a valence electron.

Within the Koopmans' theorem[20] (KT) approximation, VAEs are equal to the empty MO energies, just as the complementary IEs supplied by photoelectron spectroscopy are equal to the negative of the energies of the filled MOs. The KT approximation neglects correlation and relaxation effects, which tend to cancel out for the cations, but act in the same (stabilizing) direction for the anions. The virtual orbital energies (VOEs) calculated at the Hartree−Fock (HF) level for the neutral molecules consistently overestimate the measured VAEs by several eV.

However, it was noticed that the trends of the VOEs obtained with finite basis sets in molecules with similar structures parallel the experimental trends. In particular, Chen and Gallup[21] and Staley and Strnad[22] demonstrated that the π^*_{CC} VAEs measured in alkenes and benzenoid systems are linearly correlated to the corresponding HF or MP2 VOEs calculated with basis sets that do not include diffuse functions, and that this computational approach can be used for quantitative prediction of π^* VAEs. The same empirical scalings proved to reproduce satisfactorily

TABLE 1: Virtual Orbital Energies (VOEs) of the Neutral State of Diphenyl Disulfide and (in Parentheses) Scaled VOEs (See Text)[a]

orbital	B3LYP/6-31G*	MP2/6-31G*	expt. VAE
π^*	4.117 (4.58)	9.554 (4.76)	
π^*	3.999 (4.43)	9.336 (4.62)	4.28
σ^*_{SC}	1.471 (2.39)	5.546 (2.16)	
σ^*_{SC}	1.302 (2.26)	5.448 (2.10)	2.3
$\pi^*-\sigma^*_{SS}$	0.524 (1.63)	4.796 (1.68)	
π^*	−0.158 (1.08)	3.870 (1.08)	
π^*	−0.269 (0.99)	3.540 (0.86)	0.63
π^*	−0.308 (0.96)	3.409 (0.78)	
$\sigma^*_{SS}+\pi^*$	−1.593 (−0.07)	2.275 (−0.04)	≤0

[a] Experimental VAEs are also reported for comparison. All values are in eV.

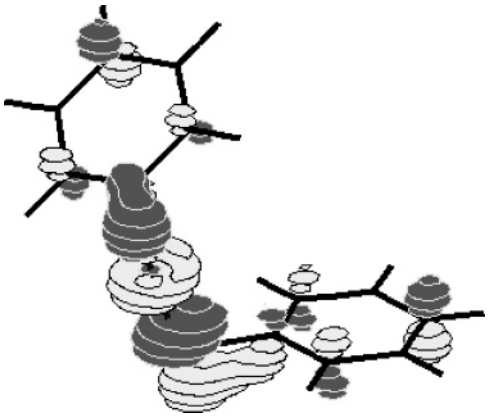

Figure 2. Representation of the SOMO of the vertical diphenyl disulfide anion, as supplied by B3LYP/6-31+G* calculations.

the π^* VAEs of carbonyl[23] and heteroaromatic[24] π-systems, and an analogous good linear correlation has also been found[25] with the Kohn−Sham VOEs supplied by B3LYP/6-31G* calculations.

Here, this approach is used to assign the features displayed by the ET spectrum of diphenyl disulfide to the corresponding anion states. Table 1 reports the VOEs calculated for the optimized geometries of the neutral state at the B3LYP and MP2 levels with the 6-31G* basis set. The corresponding values scaled with the appropriate linear equations given in refs 25 and 22, respectively, are given in parentheses. The two methods supply the same energy sequence and similar localization properties of the empty MOs, and the values of scaled VOEs (predicted VAEs) are close to each other.

Interestingly, at variance with most benzene derivatives (including mono- and dithiobenzenes) where the anion state associated with the LUMO mainly possesses ring π^* character,[26] the SOMO of the vertical ground anion state of diphenyl disulfide (as well as the LUMO of the neutral molecule) is predicted by the calculations to possess mainly σ^*_{S-S} (antibonding) character, mixed with the proper (out-of-phase) combination of the benzene e_{2u} components with maximum wave function coefficient at the substituted carbon atom. A representation of the SOMO, as supplied by the B3LYP/6-31+G* calculations (quite similar to that obtained at the B3LYP/6-31G* and MP2/6-31G* levels), is displayed in Figure 2.

Both the B3LYP and the MP2 scaled VOEs (see Table 1) are in line with the above qualitative analysis. The first VAE is predicted to be slightly negative (i.e., a slightly positive vertical electron affinity). Therefore, due to its stability (or proximity to zero energy, where it would be masked by the intense electron beam signal), the first anion state escapes detection in ETS.

The three next scaled VOEs are very close to each other at both the B3LYP and the MP2 levels, the predicted VAEs ranging from 0.8 to 1.1 eV. The first resonance displayed by the ET spectrum (centered at 0.63 eV) is thus assigned to the unresolved contributions of the corresponding three excited (essentially π^* benzene in character) anion states. The anion state associated with the LUMO counterpart, that is, the π^* benzene MO destabilized by interaction with the σ^*_{S-S} MO, is predicted to lie at about 0.6 eV higher energy. In fact, no distinct resonance is displayed by the ET spectrum in the 1.5−2 eV range. The corresponding feature in the derivatized signal is thus likely hidden by the low-energy wing of the next broad resonance.

The broad signal centered at 2.3 eV is ascribed to the unresolved contributions of the anion states associated with electron capture into the two lowest-lying σ^*_{S-C} MOs. Consistently, the corresponding σ^*_{S-C} resonances are observed at 2.7 eV in dimethyl disulfide[13] and thioanisole,[27] and at 2.3 eV in 1,4-dimethylthiobenzene.[28] It can be noted that, although the linear equations used to scale the VOEs were empirically calibrated only against π^* VAEs, scaling of the σ^*_{S-C} VOEs leads to VAEs equal to 2.3 and 2.4 eV (B3LYP) and 2.1 and 2.2 eV (MP2), in very close agreement with experiment (see Table 1).

Finally, the resonance centered at 4.28 eV arises from the two MOs deriving from the highest-lying benzene π^* (b_{2g}) MO. The scaled B3LYP VOEs (4.4 and 4.6 eV) are close to the experimental VAE, whereas (as generally found in this energy range) the scaled MP2 values (4.6 and 4.8 eV) are somewhat too high. The feature displayed at 6.2 eV is thus assigned to a core-excited resonance,[12] that is, a two-electron process where electron capture is accompanied by simultaneous excitation of a valence electron.

The first VAE can be calculated as the energy difference between the ground state anion and the neutral state (both with the optimized geometry of the neutral species). This procedure is conceptually more accurate than the KT approach. However, the description of resonance anion states (unstable with respect to electron loss) with standard bound state methods results in a difficult problem. A proper description of the spatially diffuse electron distributions of anions requires a basis set with diffuse functions.[29,30] On the other hand, as the basis set is expanded the wave function ultimately tends to describe the anion as a neutral molecule plus an unbound electron inasmuch of the continuum as the basis set can emulate (because this is the state of minimum energy), but these solutions have no physical significance with regard to the resonance process.[22,24,25,31−33] On the other hand, the VAEs calculated with basis sets that do not include diffuse functions are too high.[24,25]

The choice of a basis set that gives a satisfactory description of the energy and nature of resonance processes is therefore a delicate task. A recent study[24] of benzene and its aza, phospha, and arsa derivatives, however, has indicated that the dependence of the calculated energies and localization properties on the addition of diffuse functions to the basis set decreases with decreasing anion state energy (and consequently increasing localization of the wave function on the molecule, the part representing the continuum being correspondingly small).

Table 2 reports geometrical parameters for the neutral and anion states optimized with B3LYP calculations using the 6-31G* and 6-31+G* basis sets, the latter containing the smallest addition (s and p type placed at the non-hydrogen atoms) of diffuse functions. The two sets of parameters are quite close to each other, the main difference being the C−C−S−S

TABLE 2: Bond Distances (Å), Angles, and Dihedral Angles for the Optimized Geometries of the Neutral and Anion States of Diphenyl Disulfide

	B3LYP/6-31G*		B3LYP/6-31+G*	
	neutral	anion	neutral	anion
d(S−S)	2.1184	2.9118	2.1198	2.9019
d(S−C)	1.7958	1.7579	1.7961	1.7575
∠CSS	104.50°	104.32°	104.58°	104.04°
dihedral C−S−S−C	82.93°	81.64°	82.87°	79.81°
dihedral C−C−S−S	83.72°	103.84°	80.28°	90.62°

dihedral angle in the anion (about 104° and 91°, respectively, with the 6-31G* and 6-31+G* basis sets). The S−S bond of the neutral state is calculated to be about 0.02 Å shorter than that of dimethyl disulfide, and the C−C−S−S dihedral angle (>80°) is predicted to be nearly perpendicular to the ring planes, that is, a conformation that favors σ^*_{SS}/π^* mixing.

According to the calculations, the trans conformation (C−S−S−C dihedral angle = 180°) with the benzene rings perpendicular to the CSSC plane (which also favors σ_{SS}/π mixing) lies at 5.25 kcal/mol higher energy, being thus not significantly populated at 50 °C. The energy of the corresponding trans coplanar conformation (where σ_{SS}/π mixing is forbidden for symmetry reasons) is predicted to be even higher (9.66 kcal/mol).

Figure 3 shows the B3LYP/6-31G* energies of the neutral and anion states as a function of the S−S bond distance (with all other geometrical parameters kept equal to those of the optimized neutral state). The calculated VAE (0.006 eV, see Table 3), represented by the anion/neutral energy difference at the equilibrium S−S distance of the neutral species, is only slightly higher than that predicted by the scaled KT calculations. Inclusion of s and p diffuse functions at the non-hydrogen atoms (6-31+G* basis set) leads to a negative VAE (−0.371 eV, see Table 3), that is, a positive vertical electron affinity. The SOMO localization properties (represented in Figure 2) supplied by the 6-31+G* basis set are essentially the same as those found with the 6-31G* basis set.

In the above-mentioned study[24] of group 15 benzene derivatives, it was found that the decrease in the 6-31+G* VAE relative to the 6-31G* value is reduced with increasing stability of the anion state and that the VAE supplied by the 6-31+G* basis set is closer to experiment. For diphenyl disulfide, the difference (0.38 eV) between the 6-31G* and 6-31+G* VAEs is smaller than that (about 0.5 eV) found for phospha- and arsabenzene, where the first anion state was evaluated to lie close to zero energy.[24] This suggests that the slightly positive value (<0.1 eV) predicted by the KT scaling approach is to be considered a lower bound to the (positive) vertical electron affinity of diphenyl disulfide, the value of 0.37 eV obtained as the B3LYP/6-31+G* neutral/anion energy difference being likely more reliable.

The AEA (energy difference between the neutral state and the molecular anion, each in its optimized geometry) is predicted to be about +1 and +1.4 eV with the 6-31G* and 6-31+G* basis sets, respectively (see Table 3). Even with the 6-31+G* basis set, the SOMO of the geometry optimized anion state (where the S−S bond is about 0.8 Å longer than in the neutral state) is correctly described as a mainly σ^*_{S-S} MO. According to Rydberg electron-transfer spectroscopy data,[14] the AEA of dialkyl disulfides is slightly positive (0.1 eV). Replacement of the alkyl groups with phenyl groups would thus increase both the vertical (−1.04 eV in dimethyl disulfide[13]) and the adiabatic electron affinities by about 1 eV. In view of the importance of S−S bonds in biomolecules, it is also to be noted that the stability of the anion relative to the neutral molecule further increases in dielectric solvents. Antonello et al.[34] evaluated this effect to be about 1.7 eV for diphenyl disulfide in dimethylformamide.

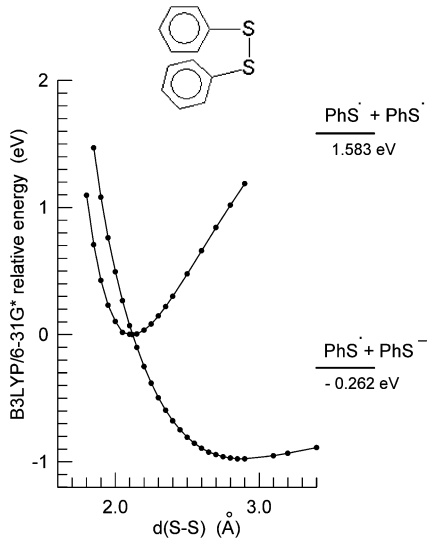

Figure 3. Potential energy curves of the neutral and anion states of diphenyl disulfide, as a function of the S−S distance.

TABLE 3: Δ Energy (eV) Relative to the Neutral State of Diphenyl Disulfide

	B3LYP/6-31G*	B3LYP/6-31+G*
$C_6H_5S-SC_6H_5$	0.00	0.00
$2C_6H_5S^\bullet$	1.583 (S−S BDE)	1.577 (S−S BDE)
$C_6H_5S-SC_6H_5^-$ (vertical)	0.006 (VAE)	−0.371 (VAE)
$C_6H_5S-SC_6H_5^-$ (optimized)	−1.057 (−AEA)	−1.382 (−AEA)
$C_6H_5S^- + C_6H_5S^\bullet$	−0.262	−0.660

The dissociation limits (represented in Figure 3) of the neutral and anion states have been calculated allowing for geometry relaxation of the fragments. The S−S bond dissociation energy (BDE) of the neutral molecule is calculated to be 1.58 eV with both basis sets (see Table 3), somewhat smaller than that (2.0 eV) obtained at the MP2/6-311G* level.[34] Comparison of the total energy of the $C_6H_5S^-$ and C_6H_5S fragments relative to that of the optimized molecular anion (see Table 3) leads to a S−S BDE of 0.795 eV (6-31G*) or 0.722 eV (6-31+G*) in the geometrically relaxed anion, in good agreement with the BDE (0.77 eV) supplied[34] by MP2/6-311G*//HF/6-311G* calculations.

The dissociation products of the anion (C_6H_5S and $C_6H_5S^-$) are predicted to be more stable (0.262 eV, 6-31G*; 0.660 eV, 6-31+G*) than the neutral state molecule in its equilibrium geometry (see Table 3). Thus, according to the calculations, there is no thermodynamic threshold for cleavage of the S−S bond upon anion formation, so that even attachment of zero energy electrons to the neutral molecule would fulfill the energy requirement for production of $C_6H_5S^-$ negative fragments.

Dissociative Electron Attachment Spectra. Figure 4 displays the total anion current (upper curve) measured at the walls of the collision chamber, as a function of the incident electron energy, in the 0−5 eV energy range. Two peaks with maxima at about 0.0 and 0.6 eV (roughly calibrated against the electron beam rise at zero energy) are observed (see Table 4), and a weak signal seems also to be present around 4 eV. The anion yield at low energy is consistent with the empty level structure deduced above from the ET spectrum and calculations. The zero

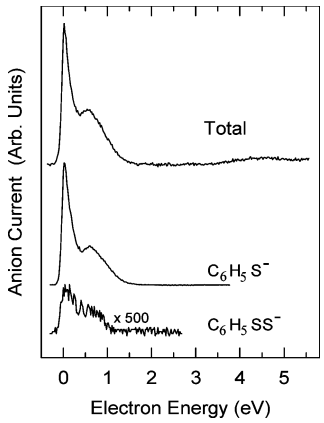

Figure 4. Total and fragment anion currents in diphenyl disulfide, as a function of the incident electron energy.

TABLE 4: Peak Energies (eV) and Relative Intensities (As Evaluated from the Peak Heights) Measured in the Total Anion Current and in the Fragment Anion Currents Observed through a Mass Filter

total anion current	fragment anion current	
peak en. (rel. int.)	peak en. (rel. int.) $C_6H_5S^-$	peak en. (rel. int.) $C_6H_5SS^-$
0.6 (35%)	0.59 (32%)	0.6
0.0 (100%)	0.02 (100%)	0.1 (0.07%)

energy peak can clearly be associated with formation of the (vibrationally excited) first anion state, while the energy of the second peak corresponds to that (0.63 eV) of the first resonance observed in the ET spectrum.

The current of anions extracted from the collision chamber and mass-selected with a quadrupole filter reveals that the total anion current is essentially completely accounted for by the $C_6H_5S^-$ fragment (see Figure 4), whose yield displays two maxima at 0.02 and 0.59 eV, calibrated against the SF_6^- peak at zero energy.

The intense zero energy peak is in line with the S−S antibonding nature of the first anion state and the results of the calculations, which predict that the energetic requirement for dissociation of the molecular anion along the S−S bond is fulfilled even at zero energy, as mentioned above. Less obviously, the $C_6H_5S^-$ fragment is also produced by dissociation of the anion states (or some of them) located at about 0.6 eV, which according to the calculations possess essentially ring π^* character. In this case, at variance with dissociation of the ground anion state, the process can be thought of as electron capture into the benzene rings, followed by intramolecular electron transfer to the S−S bond. Because of a relatively long lifetime of the benzene π^* anion states, this mechanism turns out to be efficient despite their small localization on the sulfur atoms.

The only other negative fragment detected was $C_6H_5SS^-$ (see Figure 4 and Table 4), which gives rise to two peaks at 0.1 and 0.6 eV, indicating that the ground and the first excited anion states can also follow a decay channel, which leads to dissociation of the S−C bonds. However, the $C_6H_5SS^-$ fragment is nearly 1500 times less abundant than $C_6H_5S^-$. Similarly, the DEA spectra of dimethyl disulfide[13] showed that dissociative electron attachment to the σ^*_{S-S} MO mainly leads to cleavage of the S−S bond, but a weak (2−3 orders of magnitude smaller) CH_3SS^- negative current was also observed.

A striking feature of the DEA spectra of diphenyl disulfide consists of the very large abundance of the $C_6H_5S^-$ fragment. Quantitative measurements of the (absolute or relative) dissociative cross-sections are a delicate but important aspect of DEA spectroscopy. For instance, we used such measurements as a probe for the efficiency of intramolecular electron-transfer processes in saturated and unsaturated halohydrocarbons.[25,35,36] In diphenyl disulfide, the total anion current at zero energy (essentially due only to the $C_6H_5S^-$ fragment) turned out to be about 60 times larger than that peaking at 0.75 eV in chlorobenzene and 625 times larger than that peaking at 1.54 eV in *tert*-butyl chloride,[35] as evaluated from the peak heights. Although there could be larger differences in pressure (measured in the main vacuum chamber) for the less volatile diphenyl disulfide, the effective cross-section, convoluted with our electron beam energy distribution, would tend to be underestimated. The absolute cross-section for *tert*-butyl chloride was reported[37] to be 3.18×10^{-18} cm^2, which leads to 2.0×10^{-15} cm^2 for $C_6H_5S^-$ at zero energy. This very large dissociative cross-section for attachment of thermal electrons in the gas phase is in qualitative agreement with the very large rate constant for the cleavage of the S−S bond found in solution upon electrochemical reduction.[34]

Conclusions

Disulfide bonds are involved in conformational stability and biological activity of proteins and in protein folding. The study of the electron-acceptor properties of disulfides in the gas phase and characterization of their lowest-lying anion states, as well as their dissociative decay channels, may serve as a model for the understanding of the reductive process in the larger biological systems. The absence of a corresponding resonance in the ET spectrum of diphenyl disulfide indicates that the first anion state lies very close to zero energy, where it would be obscured by the intense electron beam signal, or is more stable than the neutral state molecule. In agreement, the virtual orbital energies of the neutral molecule, obtained at the MP2/6-31G* and B3LYP/6-31G* levels and scaled with empirical linear equations, nicely account for the ET spectral features and predict a slightly positive (about 0.05 eV) vertical electron affinity. A somewhat higher value (0.37 eV) is obtained with B3LYP/6-31+G* calculations as the neutral/anion total energy difference.

The stability of the first anion state is also confirmed by the DEA spectrum. The anion current, recorded as a function of the incident electron energy, displays an intense peak at zero energy essentially due to the $C_6H_5S^-$ negative fragments. Thus, there is a large cross-section for capture of thermal electrons, followed by rapid dissociation of the molecular anion along the S−S bond. The experimental findings are accounted for by the calculations: the first anion state is predicted to be largely localized at the S−S bond in an antibonding manner, and the two fragments to be thermodynamically stable with respect to the molecular anion formed at zero energy.

The results from this study may also provide insight into the reaction between the disulfide and the dimer rows on the silicon (001) surface.[9] Although the silicon−sulfur bonding mechanism can be explained in terms of a polarization of charge between the "up" and "down" atoms in the tilted silicon dimer allowing nucleophilic attack at the "down" atom,[10] the electron-acceptor properties and the dissociative electron attachment spectra (DEAS) of diphenyl disulfide discussed above would also admit the hypothesis of a more concerted mechanism for this reaction where electron transfer would not be solely from a sulfur atom to silicon but also from the Si−Si pseudo-π to the S−S σ^* LUMO.

Acknowledgment. A.M. thanks the Italian Ministero dell'Istruzione, dell'Università e della Ricerca, for financial support.

References and Notes

(1) Chen, J.; Song, J.-L.; Zhang, S.; Wang, Y.; Cui, D.-F.; Wang, C. C. *J. Biol. Chem.* **1999**, *274*, 19601.

(2) Barbirz , S.; Jakob, U.; Glocker, M. O. *J. Biol. Chem.* **2000**, *275*, 18759.

(3) Velázquez, I.; Reimann, C. T.; Tapia, O. *J. Phys. Chem. B* **2000**, *104*, 2546.

(4) Dai, S.; Schwendtmayer, C.; Schürmann, P.; Ramaswamy, S.; Eklund, H. *Science* **2000**, *287*, 655.

(5) Nakamura, H.; Nakamura, K.; Yodoi, J. *Annu. Rev. Immunol.* **1997**, *15*, 351.

(6) El Hanine Lmoumène, C.; Conte, D.; Jacquot, J.-P.; Houée-Levin, C. *Biochemistry* **2000**, *39*, 9295.

(7) Favaudon, V.; Tourbez, H.; Houée-Levine, C.; Lhoste, J.-M. *Biochemistry* **1990**, *29*, 10978.

(8) Zubarev, R. A.; Kruger, N. A.; Fridriksson, E. K.; Lewis, M. A.; Horn, D. M.; Carpenter, B. K.; McLafferty, F. W. *J. Am. Chem. Soc.* **1999**, *121*, 2857.

(9) Coulter, S. K.; Schwartz, M. P.; Hamers, J. H. *J. Phys. Chem. B* **2001**, *105*, 3079.

(10) Wayner, D. D. M.; Wolkow, R. A. *J. Chem. Soc., Perkin Trans. 2* **2002**, 23−34.

(11) Sanche, L.; Schulz, G. J. *J. Phys. Rev. A* **1972**, *5*, 1672.

(12) Schulz, G. J. *Rev. Mod. Phys.* **1973**, *45*, 378, 423.

(13) Modelli, A.; Jones, D.; Distefano, G.; Tronc, M. *Chem. Phys. Lett.* **1991**, *181*, 361.

(14) Carles, S.; Lecomte, F.; Schermann, J. P.; Desfrançois, C.; Xu, S.; Nilles, J. M.; Bowen, K. H.; Bergès, J.; Houée-Levin, C. *J. Phys. Chem. A* **2001**, *105*, 5622.

(15) Modelli, A.; Jones, D.; Distefano, G. *Chem. Phys. Lett.* **1982**, *86*, 434.

(16) Johnston, A. R.; Burrow, P. D. *J. Electron Spectrosc. Relat. Phenom.* **1982**, *25*, 119.

(17) Modelli, A.; Foffani, A.; Scagnolari, F.; Jones, D. *Chem. Phys. Lett.* **1989**, *163*, 269.

(18) Frisch, M. J.; Trucks, G. W.; Schlegel, H. B.; Scuseria, G. E.; Robb, M. A.; Cheeseman, J. R.; Zakrzewski, V. G.; Montgomery, J. A., Jr.; Stratmann, R. E.; Burant, J. C.; Dapprich, S.; Millam, J. M.; Daniels, A. D.; Kudin, K. N.; Strain, M. O.; Farkas, O.; Tomasi, J.; Barone, V.; Cossi, M.; Cammi, R.; Mennucci, B.; Pomelli, C.; Adamo, C.; Clifford, S.; Ochterski, J.; Petersson, G. A.; Ayala, P. Y.; Cui, Q.; Morokuma, K.; Malick, D. K.; Rabuck, A. D.; Raghavachari, K.; Foresman, J. B.; Cioslowski, J.; Ortiz, J. V.; Stefanov, B. B.; Liu, G.; Liashenko, A.; Piskorz, P.; Komaromi, I.; Gomperts, R.; Martin, R. L.; Fox, D. J.; Keith, T.; Al-Laham, M. A.; Peng, C. Y.; Nanayakkara, A.; Gonzalez, C.; Challacombe, M.; Gill, P. M. W.; Johnson, B.; Chen, W.; Wong, M. W.; Andres, J. L.; Head-Gordon, M.; Replogle, E. S.; Pople, J. A. *Gaussian 98*, revision A.6; Gaussian, Inc.: Pittsburgh, PA, 1998.

(19) Becke, A. D. *J. Chem. Phys.* **1993**, *98*, 5648.

(20) Koopmans, T. *Physica* **1933**, *1*, 104.

(21) Chen, D. A.; Gallup, G. A. *J. Chem. Phys.* **1990**, *93*, 8893.

(22) Staley, S. S.; Strnad, J. T. *J. Phys. Chem.* **1994**, *98*, 161.

(23) Modelli, A.; Martin, H.-D. *J. Phys. Chem. A* **2002**, *106*, 7271.

(24) Modelli, A.; Hajgató, B.; Nixon, J. F.; Nyulászi, L. *J. Phys. Chem. A* **2004**, *108*, 7440.

(25) Modelli, A. *Phys. Chem. Chem. Phys.* **2003**, *5*, 2923.

(26) Modelli, A. *Trends Chem. Phys.* **1997**, *6*, 57.

(27) Guerra, M.; Distefano, G.; Jones, D.; Colonna, F. P.; Modelli, A. *Chem. Phys.* **1984**, *91*, 383.

(28) Modelli, A.; Distefano, G.; Guerra, M.; Jones, D.; Rossini, S. *Chem. Phys. Lett.* **1986**, *132*, 448.

(29) Hehre, W. J.; Radom, L.; Schleyer, P. v. R.; Pople, J. A. *Ab Initio Molecular Orbital Theory*; J. Wiley: New York, 1986.

(30) Dunning, T. H., Jr.; Peterson, K. A.; Woon, D. E. Basis Sets: Correlation Consistent Sets. In *The Encyclopedia of Computational Chemistry*; Schleyer, P. v. R., Ed.; John Wiley: Chichester, 1998.

(31) Heinrich, N.; Koch, W.; Frenking, G. *Chem. Phys. Lett.* **1986**, *124*, 20.

(32) Guerra, M. *Chem. Phys. Lett.* **1990**, *167*, 315.

(33) Chao, J. S.-Y.; Falcetta, M. F.; Jordan, K. D. *J. Chem. Phys.* **1990**, *93*, 1125.

(34) Antonello, S.; Daasbjerg, K.; Jensen, H.; Taddei, F.; Maran, F. *J. Am. Chem. Soc.* **2003**, *125*, 14905.

(35) Modelli, A.; Venuti, M.; Szepes, L. *J. Am. Chem. Soc.* **2002**, *124*, 8498.

(36) Modelli, A.; Jones, D. *J. Phys. Chem. A* **2004**, *108*, 417.

(37) Pearl, D. M.; Burrow, P. D. *J. Chem. Phys.* **1994**, *101*, 2940.